Analysis of Lateral Redistribution of a Monoclonal Antibody Complex Plasma Membrane Glycoprotein which Occurs during Cell Locomotion

Akira Ishihara,* Bruce Holifield,* and Ken Jacobson*‡

*Laboratories for Cell Biology, Department of Cell Biology and Anatomy, and ‡Cancer Research Center, School of Medicine, University of North Carolina at Chapel Hill, Chapel Hill, North Carolina 27599

Abstract. The lateral redistribution of a major murine glycoprotein, GP80, was studied on locomoting fibroblasts, using rhodamine-conjugated mAbs and ultra-low light level digitized fluorescence microscopy. Confirming an earlier study (Jacobson, K., D. O'Dell, B. Holifield, T. L. Murphy, and J. T. August. 1984. *J. Cell Biol.* 99:1613–1623), the distribution of GP80 was coupled with cell locomotion; motile cells exhibited a gradated distribution of the GP80-mAb complex over the cell surface, increasing from the front to the rear, whereas stationary cells exhibited a nearly uniform GP80 distribution. By monitoring locomoting single cells, we found the gradated fluorescence distribution to be maintained as an approximate steady state. Newly extended leading edges were almost devoid of the fluorescence labeling. This was strikingly demonstrated in prechilled cells in which the extension of fluorescence-free leading edges caused a pronounced boundary between fluorescent and nonfluorescent zones. Subsequently this boundary eroded gradually in a manner consistent with diffusional relaxation. Evidence indicated that the GP80 redistribution was primarily caused by the lateral motion of GP80 in the plasma membrane and not via intracellular membrane traffic. Two cell locomotion models which, in principle, could account for the GP80 redistribution were tested: the retrograde lipid flow (RLF) model (Bretscher, M. S., 1984. *Science (Wash. DC).* 224:681–686) and an alternative hypothesis, the retraction-induced spreading (RIS) model. The predictions of these models were simulated by computer and compared with experiment to assess which model was more appropriate. Whereas both models predicted steady-state gradients similar to the experimental result, only the RIS model predicted the lack of retrograde movement of the fluorescent boundary.

FIBROBLASTIC cells move in a series of highly complex locomotory activities. Cells extend leading lamellipodia, form new attachments with substratum, pull the cell body forward, and retract their trailing edges (Abercrombie, et al., 1970*a* and *b*). Little is known about molecular mechanisms underlying these dynamic activities.

We have been investigating the behavior of plasma membrane components during cell locomotion using a major membrane glycoprotein, GP80, as a marker. GP80 (also referred to as pgp-1) was identified by a mAb raised against mouse fibroblasts (Hughes and August, 1981; Trowbridge et al., 1982). The antigen has been characterized biochemically and genetically (Hughes et al., 1981 and 1982; Colombatti et al., 1982). GP80 is present in high copy number, about 10^6/cell. Fluorescent antibody labeling persists for long times (~100 h) without being appreciably internalized and does not appear to affect cell locomotion (Jacobson et al., 1984*b*). Previously we showed by indirect immunofluorescence microscopy of fixed cells that GP80 exhibits a gradated distribution in locomoting cells but not in stationary cells (Jacobson et al., 1984*b*).

Various cell locomotion mechanisms have been proposed and some of them predict a gradated distribution of membrane proteins in locomoting cells. In the present study, the redistribution of GP80 labeled with rhodamine-conjugated mAb was observed and measured quantitatively at the level of single living cells, using ultra-low light level digitized fluorescence microscopy (DFM;[1] DiGiuseppi et al., 1985; Kapitza et al., 1985; Arndt-Jovin et al., 1985). The DFM system utilizes very low excitation light, reducing possible phototoxic effects, and allows acquisition of sequential averaged images of a single motile cell with little photobleaching of the specimen. The redistribution of GP80 in motile mouse fibroblasts was then compared with the quantitative predic-

Address correspondence to Professor Ken Jacobson.

1. *Abbreviations used in this paper*: *D*, diffusion coefficient; DFM, digitized fluorescence microscopy; F-anti-GP80, fluorescein-conjugated monoclonal anti-GP80 antibody; R-anti-GP80, rhodamine-conjugated monoclonal anti-GP80 antibody; RIS, retraction-induced spreading; RLF, retrograde lipid flow.

tions of the cell locomotion models produced by computer simulations.

Models for Membrane Protein Redistribution during Cell Locomotion

Two extreme quantitative hypotheses have been proposed which predict a gradated distribution of membrane proteins in locomoting cells. The retrograde lipid flow (RLF) hypothesis (Bretscher, 1984) derives from the following observations. (*a*) Particles attached to the dorsal or ventral surface of substratum-attached cells move from the leading edge area centripetally toward central surface areas (Abercrombie et al., 1970*c*; Harris and Dunn, 1972). Membrane proteins, initially distributed uniformly, are transported after crosslinking to form patches, away from the leading edges and collect in the rear portion of the cell or over the nucleus (DePetris and Raff, 1973; Vasilev et al., 1976). (*b*) Recycling proteins such as the low density lipoprotein receptor and the transferrin receptor are inserted at the leading edges of some of locomoting cells (Bretscher, 1983), as are some newly synthesized virus proteins (Marcus, 1962; Bergmann et al., 1983). The model postulates the polarized recycling of membrane lipids (see also Fig. 7 *a*). According to this model, membrane inserted at the leading edge serves as a source while concommitant endocytosis over the cell surface serves as a sink, and the source and sink are coupled by a front-to-rear lipid flow. Membrane insertion at the front of the cell causes an extension of the leading edge, an obligatory step in cell translocation. The RLF model makes specific predictions about how monomeric and aggregated membrane proteins are influenced by the lipid flow. Whether or not a particular component is carried rearward with the flow is determined by the relative values of the flow velocity and the diffusion coefficient of the component. Components with a small lateral diffusion coefficient relative to the lipid flow velocity will undergo appreciable retrograde transport.

The second hypothesis represents an amalgamation of observation and theory. The key observation is that in locomoting cells the total surface area appears to be constant and that the extension of leading edges is often coupled with the retraction of trailing edges (referred as retraction-induced spreading) (Chen, 1979, 1981*a* and *b*; Dunn, 1980). This suggests that the membrane constituting newly extended surface area is obtained from a forward flow of plasma membrane originating from the reserve membrane accumulated when trailing edges retract. A similar mechanism has been suggested for cells spreading on the substrate from villous, round forms (Erickson and Trinkaus, 1976). Second, Jacobson et al. (1984*a*) proposed that the low lateral diffusion coefficient of GP80 in the plasma membrane, relative to those of proteins reconstituted in bilayers (Vaz et al., 1984; Jacobson, 1983), could be explained if the GP80 molecules were transiently anchored to peripheral structures, i.e., membrane-associated cytoskeleton or extracellular matrix. The gradated distribution of transiently anchored membrane proteins in locomoting cells would arise if during the forward flow of membrane, molecules such as GP80 were not carried along by the forward flow, resulting in a relatively higher density of GP80 in the rear portion of the cell (see also Fig. 9 *a*). This situation has been modeled by Dembo and coworkers (1981) for the formally equivalent case where certain membrane proteins are involved in making transient bonds to the substratum. This hypothesis was termed the reaction-convection model and it predicts the formation of density gradients for such membrane proteins in locomoting cells. We shall call our amalgamated model the retraction-induced spreading (RIS) model.

These models fundamentally differ in that one, the RLF model, derives additional membrane for leading edge extension from internal pools, whereas the other, the RIS model, utilizes existing surface membrane reservoirs in the form of folds to provide the plasma membrane to cover the extending leading edge. The models are also diametrically opposed with respect to the direction of membrane flow and the fact that proteins in the RLF model are directly "pushed" by the flow, whereas in the RIS model they are protected from the flow due to transient anchorage to structures peripheral to the membrane.

Materials and Methods

Antibodies

AMF-15 mAb (Hughes et al., 1981), an IgG which binds GP80, was obtained from J. T. August, the Johns Hopkins University, and isolated from mouse ascites fluid as previously described (Jacobson et al., 1984*b*). Dichlorotriazinylaminofluorescein (DTAF) and lissamine rhodamine B sulfonyl chloride were obtained from Research Organics, Cleveland, OH, and Molecular Probes, Inc., Junction City, OR, respectively. DTAF (Jacobson et al., 1984*b*) and lissamine rhodamine (Ishihara et al., 1987) were conjugated to the antibodies as described before. The dye/protein molar ratio ranged from 1.1 to 1.6. Specificity of the conjugated antibodies was tested as described before (Jacobson et al., 1984*b*) with BALB/c/3T3 cells which express an allelic form of GP80 that AMF-15 does not recognize (Hughes et al., 1981).

Cultured Cells

Stock cultures of C3H/10T1/2 cells were obtained from American Type Culture Collection, Rockville, MD. Cells were maintained in basal medium Eagle (BME) with Earl's Salts (Gibco, Grand Island, NY) supplemented with 5 or 10% FBS as described previously. Cells in early passage (p9–14) were used. Cells were plated onto 12-mm square cover slips and used 36–60 h after plating for the experiments.

Direct Immunofluorescence of Living Cells

Cells on a coverslip were washed in PBS and stained with 100–200 μg/ml rhodamine-conjugated anti-GP80 antibody (R-anti-GP80) for 10 min at room temperature by inverting the coverslip and placing it on a 20-μl droplet of antibody solution in a humidified atmosphere. After labeling, the coverslip was floated by flooding the culture dish with PBS, the cells were washed in PBS, and mounted on a metal slide with BME medium containing 10 mM Hepes buffer, pH 7.4. For certain experiments cells were preincubated in BME medium containing 10% FBS and 10 mM Hepes buffer at 4°C for >3 h.

Low Light Level Digital Fluorescence Microscopy

A Zeiss IM35 inverted microscope equipped with mercury lamp, epifluorescent illumination, and 63× Neofluor objective lens (1.25 NA) was used for observation. To preserve cell function while still providing an adequate signal-to-noise ratio in the image, we minimized excitation energy by attenuating the Zeiss 100 W Mercury burner with a filter ranging from 0.6 to 1.0 in neutral density. Power through the objective at 546 nm was measured to be in the range of 0.16–0.44 μW using a Coherent laser power meter (model 815 PS, Newport Corp., Fountain Valley, CA). Images were recorded with Model 66 ISIT (Intensifier Silicon-Intensifier Target) camera (Dage-MTI, Michigan City, IN) and digitized on line using circuitry from Imaging Technology, Woburn, MA, in a host PDP 11/23 microcomputer (Digital Equipment Corp., Maynard, MA); the images were "grabbed" as an array of 256 × 256 pixels with 256 gray levels. Typically 256 video frames were averaged within 9 s to improve the signal-to-noise ratio and stored as one image. The ISIT camera was used in manual mode with fixed

high voltage and video gain, so that the sensitivity of the camera was kept constant. Further details of the DFM system are described elsewhere (DiGuiseppi et al., 1985). Phase-contrast images were also taken with the same camera in automatic mode. Photographs of video images were taken with a video film camera (Celtic Technology, Woodland Hill, CA).

For the observation of locomoting cells, the specimens were kept at 37°C using an air curtain incubator (model 279, Sage Instruments, Cambridge, MA) coupled to a plexiglass chamber. Temperature in the chamber was monitored with a thermocouple. The process of cell locomotion was analyzed with a time lapse video cassette recorder (TC 3800 M, RCA, Lancaster, PA) by recording phase contrast images of cells.

Video Image Analysis

Image files were first corrected for shading, which is the fall off of response toward the edges of the field. The shading correction was accomplished by numerically dividing each image by an image taken of a featureless, uniformly illuminated scene (Benson et al., 1985). The linearity of the imaging system with respect to fluorescence emitted by the specimen was verified by recording images of a uniform dihexadecylindocarbocyanine (diI-C_{16}[3]) film (Derzko and Jacobson, 1980) illuminated by increasing excitation intensities. Software was written to obtain "slice profiles" consisting of a plot of the pixel gray level vs. position. Normally 10–20 adjacent profiles were averaged. The profiles were taken from the front to the rear of the cells along the direction of motility. To obtain the averaged gradient from several cells, we first corrected the profiles by subtracting the background and then normalized before averaging so that all the profiles were given equal weight.

Two-Color Anti-GP80 Labeling

To estimate the amount of newly appearing anti-GP80 binding sites, C3H/10T1/2 cells were stained in three ways. Initially cells were kept in the cold for 3 h. First, cells were stained with 100 μg/ml rhodamine-conjugated anti-GP80 (R-anti-GP80) and then immediately stained with 100 μg/ml F-anti-GP80 antibody. Second, cells were stained with R-anti-GP80, put back into BME growth medium, incubated for 1 h, and stained with F-anti-GP80. Third, cells were stained with F-anti-GP80 alone. The fluorescence intensity of stained cells was measured by DFM. The averaged fluorescence intensity of each cell was measured over a 20 × 20 pixel (9.1 μm × 6.6 μm) area on the cell surface. The average fluorescence intensity was obtained from each of 10 cells randomly chosen in each specimen, and the mean of these values were calculated. Because the sensitivity of the video camera varies with emission wavelength and the amount of dye per antibody molecule is different between R-anti-GP80 and F-anti-GP80, the measured intensities of the two colors are not readily comparable. Therefore the relative fluorescence intensity was obtained by comparing with the intensity of the cells which were fully stained using only R-anti-GP80 or F-anti-GP80.

Computer Simulation of One-Dimensional Models

Computer simulation of GP80 redistribution was carried out on a Sun-3 Workstation computer (Sun Microsystems Inc., Mountain View, CA). The method was basically according to Berg (1983). A linear array of 100 adjacent bins of width 0.5 μm was assumed to represent position along the cell axis. Membrane protein molecules were represented by a large number of particles (in most cases, 10,000) which were distributed into the bins and were moved according to the following rules. For lateral diffusion each particle was transferred randomly to one of the two adjacent bins. In each end bin of the array, outward movements of particles were reflected by the boundary. This operation was repeated successively at appropriate time intervals to simulate the time evolution of a distribution under the influence of diffusion. The interval (τ) was calculated according to the equation $\tau = \delta^2/2D$, where δ is the interbin distance and D is the one-dimensional diffusion coefficient of the protein in question; thus, for example, moving the particles randomly to the adjacent bins every 3.9 s corresponds to a D of 3.2×10^{-10} cm^2/s. To simulate the membrane proteins being carried along with a bulk membrane flow, each particle was moved to the next bin on the downstream side. The frequency of this operation was determined by the flow velocity (V_f) to be simulated. For example, to simulate a flow velocity of 0.5 μm/min superimposed on random diffusion of the proteins characterized by $D = 3.2 \times 10^{-10}$ cm^2/s, one flow step of $\delta = 0.5$ μm was introduced every 58.5 s (i.e., one flow step per 15 diffusional steps). Particles in the end bin were not moved, resulting in an accumulation in this bin. In some cases, we assumed that all proteins were transiently anchored to peripheral structure for short "dwell times" and that only when the protein was unanchored was it subject to the flow. Because we assumed that the population of the protein was equally anchored, 95% anchoring meant that each protein was anchored 95% of the time. Therefore, when a convective flow was applied to a protein population that was 95% anchored, we included the effect of the flow as operating on all proteins but with flow velocity reduced to 5% of the original value. Tail retraction was simulated as a shortening of a portion of the cell with the retraction site positioned in the rear half (bins from No. 1 to No. 51, with bin No. 1 located at the tail end). Then, the number of bins was reduced from 51 to 50, and the particles that were present in the 51 bins were redistributed in the remaining 50 bins in proportion to the number of particles in the original distribution. The leading edge extension was simulated by adding one empty bin to the front of the cell. In the RIS model, the rate of leading edge extension was always coupled with the rate of tail retraction, and these rates were determined by the frequency of the operation. The operations for diffusion, flow, retraction, and extension were combined depending on models and repeated many times. Steady state was judged to be achieved when the change in the distribution was small after two successive operations. To obtain smooth distributions, a number (10–20) of simulations were run for each case and averaged.

Results

DFM Can Be Used to Observe GP80 Distribution in Living Cells

Murine fibroblast C3H/10T1/2 cells were stained directly with R-anti-GP80 and the distribution of GP80 was observed in locomoting cells by DFM. Labeling with the antibody did appear to not affect cell locomotion activities. The labeled cells displayed normal locomotory activities such as leading edge extension, ruffling, and trailing edge retraction. Because of its high sensitivity, the DFM system could be used to record >10 fluorescence images of single cells without significant fading. (It was estimated that the decrease in fluorescence intensity due to fading was ~1% for each image acquired.) However, we found that prolonged exposure (2–3 min) to even this minimal excitation often caused the cessation of leading edge extension. The effect appeared to be limited only to the exposed cells as the unexposed cells in the same specimen continued to extend leading edges. When the total exposure was minimized (lower intensity, <1 min of exposure in total), no effect was observed. Therefore the experiments were carried out in this range of exposure.

GP80 Distribution is Coupled to Cell Locomotion

Fig. 1 *b* shows one example of the fluorescence distribution in locomoting cells. The staining was diffuse but gradated; there was very little fluorescence on leading edges and a high intensity of fluorescence near trailing edges (compare to phase image, Fig. 1 *a*) resulting in a gradient in fluorescence. The gradient appears to be due to a genuine increase in the membrane concentration of GP80 toward the rear of the cell and not generally due to a cell morphology artefact. The strongest evidence supporting this assertion comes from the fact that lipid analogue probes such as diI-C_{16}(3) show no gradient in locomoting cells (Jacobson et al., 1984*b*). In addition, two other membrane proteins, Thy-1 and H-2 (major histocompatibility antigen), did not show gradated distributions (Ishihara et al., 1988). Some of the cells extended lamellipodia from two or three sites simultaneously. In those cells the fluorescence intensity was very weak at all the active edges (see Fig. 4). The magnitude of the fluorescence gradients varied considerably (see Fig. 3). Fibroblasts were reincubated at 4°C for >3 h to inhibit locomotion. These

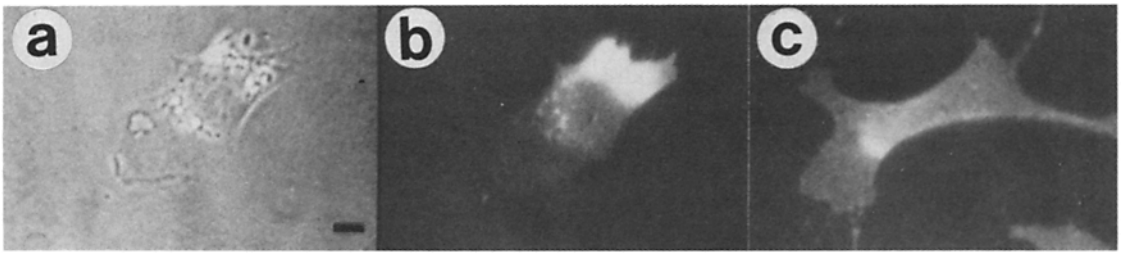

Figure 1. Gradated GP80 distribution in locomoting cells and uniform distribution in stationary cells. (*a*) Phase-contrast image of a locomoting C3H/10T1/2 mouse fibroblast. (*b*) Fluorescent image of the same cell stained with R-anti-GP80. (*c*) Fluorescent image of a stationary fibroblast stained with R-anti-GP80. The cells were preincubated at 4°C for 3 h to arrest locomotion. Bar, 10 μm.

cells showed a nongradated staining pattern when labeled with anti-GP80 (Fig. 1 *c*). When these cells were incubated for 1 h at 37°C and stained with R-anti-GP80, they regained a gradated distribution of fluorescence (data not shown).

GP80 Distribution in Continuously Locomoting Cells: Maintenance of a "Steady State" Gradient

C3H/10T1/2 cells were stained with R-anti-GP80 and their

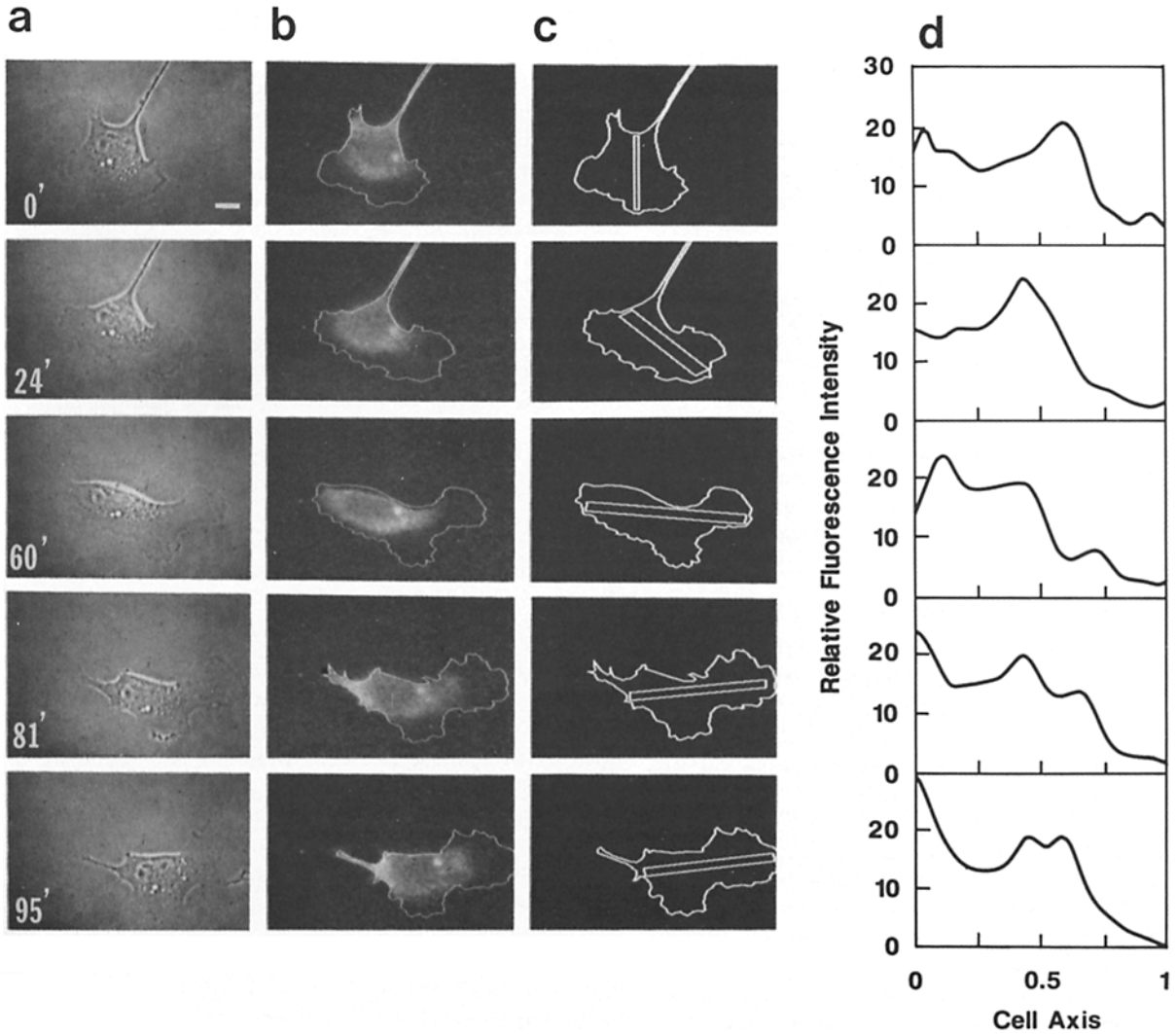

Figure 2. "Steady state" gradated GP80 distribution in locomoting cells. Columns *a* and *b* show a time sequence of phase-contrast images and the corresponding fluorescent images of locomoting fibroblast stained with R-anti-GP80 (160 μg/ml), respectively. White lines on the fluorescent images indicate cell edges obtained from the corresponding phase-contrast images. Diagrams in column *c* show the cell shapes and the rectangular areas from which slice profiles (*d*) of fluorescence intensity were taken. A number (10–20) of fluorescence profiles parallel to the long axis were obtained in the rectangular areas and averaged to give the profiles in column *d*. The scale of the ordinate is not an absolute distance but is referred to the length of the rectangle used for each time point. Bar, 10 μm.

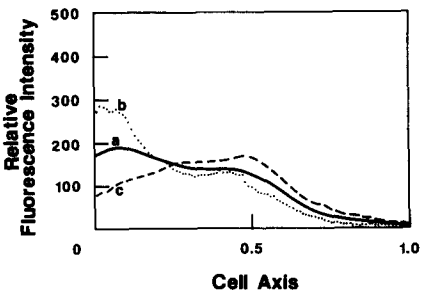

Figure 3. The mean GP80 gradient. A mean profile of the gradated fluorescence distributions was obtained from profiles of seven cells whose shapes were approximately rectangular. Abscissa indicates the relative location on the cell axis from the rear end to the front end of cell. Ordinate indicates the relative fluorescence intensity in arbitrary units. The intensity profile was corrected first by the subtraction of the background and then by the normalization to give each of the profiles an equal weight before the averaging. Line *a* shows the average of the seven profiles. Lines *b* and *c* show the average of the three steepest profiles and of the three shallowest profiles, respectively.

locomotion was observed at 37°C. Fig. 2 shows one example of the phase contrast and corresponding fluorescence images of locomoting cells. The locomotory behavior of C3H/10T1/2 cells was similar to that of chicken embryo fibroblasts which have been extensively studied. The extension speed of the leading edges was variable in time and among different cells; for example, the speeds measured in three cells ranged from 0.16 to 0.85 μm/min. The retraction of the trailing edge was complex but could be classified into two modes of activity. The first mode consisted of a shrinking of trailing portion of the cell in which the distal point remained at nearly the same position. The area between the lateral edges decreased, resulting in the formation of a thinner tail. The second activity consisted of detachment of the trailing tip and rapid retraction of the trailing region. An example is given in the time series shown in Fig. 2 and demonstrates shrinking of the trailing region and subsequent detachment of the tip of the tail.

The R-anti-GP80 fluorescence labeling pattern as a whole translocated as the cells advanced, but the distribution of fluorescence remained gradated. When new lamellae were extended, very little fluorescence was detected in the newly extended area. The posterior part of cells maintained a high intensity of fluorescence resulting in the maintenance of the pronounced gradient. During the first mode of retraction (shrinkage of trailing edge), the fluorescence intensity in the trailing edge often increased (see Fig. 5 and below). To obtain a quantitative estimation of the gradient magnitude, we took profiles of the fluorescence intensity from the DFM images along a cell axis aligned with the direction of locomotion. As shown in Fig. 2 *c*, 10–20 profiles along the selected cell axis were taken in the region outlined by the box, and these were averaged. The profiles taken at various times (Fig. 2 *d*) show that the shapes of the gradients were qualitatively similar. The front third of the cell was nearly fluorescence free, followed by a steep rise in fluorescence with the rear half of the cell having nearly constant intensity, with the exception of the dip over the "nuclear" mound, which was observed occasionally but not always (compare Fig. 2 with Fig. 3). Several other profiles with different axis orientations were also taken for each fluorescence image (in Fig. 2). The shapes of the profiles were qualitatively similar for axes oriented at ±18 degrees to the axes used in Fig. 2. This series of profiles, typical of several examined in detail, indicates that in continuously locomoting cells, the GP80-mAb lateral distribution maintains similar shapes over time, suggesting the term "steady state gradient."

The fluorescence redistribution was also observed when the cells were cooled from 37°C to room temperature and ceased to locomote. The fluorescence gradients remained visible although somewhat diminished for time in excess of 2 h, indicating the relaxation of the gradient, presumably via lateral diffusion of GP80, was a very slow process. Considering cell lengths of 40–80 μm of the GP80-mAb complexes, diffusion coefficients $\sim 10^{-10}$ cm²/s are indicated by such observations. The root mean square distance diffused in two dimensions in 2 h is 17 μm given a D of 10^{-10} cm²/s, whereas it is 170 μm when $D = 10^{-8}$ cm²/s.

Measurements of Steady State Gradients

Steady state gradients were measured quantitatively for subsequent comparison with theoretical models. Locomoting C3H/10T1/2 cells were stained with R-anti-GP80, and fluorescence cross-sectional profiles were taken along the cell axis in the direction of motion. We chose seven cells whose morphologies were approximately rectangular and took the mean of the profiles. The average of the three steepest and three shallowest profiles are also shown in Fig. 3. The magnitude of the gradients varied among the cells. The presumption is that the steepest gradients reflect those cells in the selected collection which exhibit the highest locomotory activity. The length of the cell axis ranged from 50 to 118 μm. There was no apparent correlation between the steepness of the gradient and the cell length.

Cells Spreading after Temperature Increase Show Development of a Gradated Distribution

We monitored how the redistribution of the GP80-mAb complex developed from the uniform distribution on prechilled cells to the gradated distribution on warmed cells. Cells were incubated at 4°C for 4 h and stained with R-anti-GP80. The cells exhibited much reduced locomotion and the fluorescence distribution was nearly uniform over the cell surface as noted above. Upon raising the temperature to 37°C, the cells started to extend new leading edges (Fig. 4). We often observed that cells extended a multiple number (two to five) of leading edges nearly simultaneously (Fig. 4, *black arrows* [5 min]). For the first 30–60 min, the leading edges continued to extend but the cells displayed no retraction activity, and no net translocation of the cell body was seen.

The corresponding fluorescence images of the cells show that there was very little fluorescence intensity in any of the newly extended leading edges (compare fluorescence and phase images of Fig. 4 [5 min]). As a result, fluorescence boundaries were formed between the fluorescent and nonfluorescent regions (for example, see white arrows in the right micrograph of Fig. 4 at 17′). The fluorescence boundary was the sharpest immediately after the first lamellar extension. With time the boundary became more diffuse (white arrowheads in the right micrograph of Fig. 4 at 45′) as fluorescence

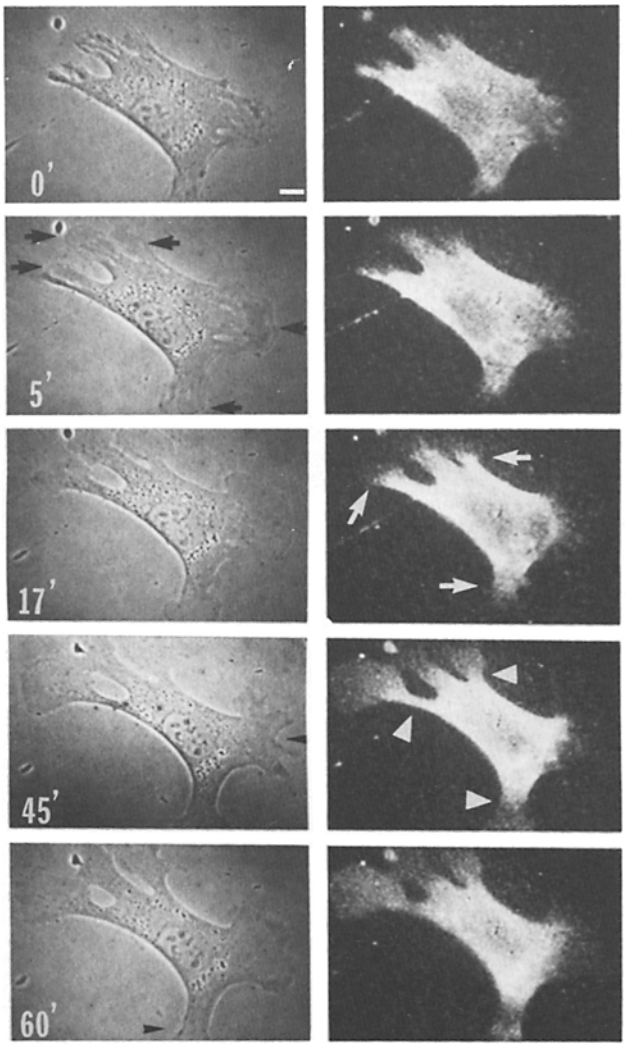

Figure 4. Redistribution of GP80 in spreading cells. The left column shows phase-contrast images of a fibroblast that was preincubated at 4°C for 3 h, labeled with R-anti-GP80 (190 μg/ml), and warmed to 37°C at time zero. The right column shows the corresponding fluorescent images of the R-anti-GP80 labeling. Note that the cell extended leading edges at several sites simultaneously (black arrows in phase image at 5′) and that the fluorescence was absent in those newly extended areas, resulting in formation of fluorescence boundary (white arrows in fluorescence image at 17′). At 45 min the boundary became more diffuse (white arrowheads in fluorescence image). After the extension reached the maximum, a few retractive motions were observed (black arrowheads in phase images at 45′ and 60′). Bar, 10 μm.

intensity increased in the newly extended lamellae (compare lamellae marked by white arrows in Fig. 4 (17′) with corresponding lamellae at 45′ and 60′). Note that the boundary position never appeared to move rearward as the extension continued. Also, some retraction was evident at 45 and 60 min (black arrowheads in phase images).

This redistribution process after leading edge extension was analyzed in detail for several cells. One example is shown in Fig. 5. Upon an increase in temperature this cell extended leading edges in two opposite directions, but the left one ceased extending shortly after the observation began whereas the right one continued to extend almost linearly

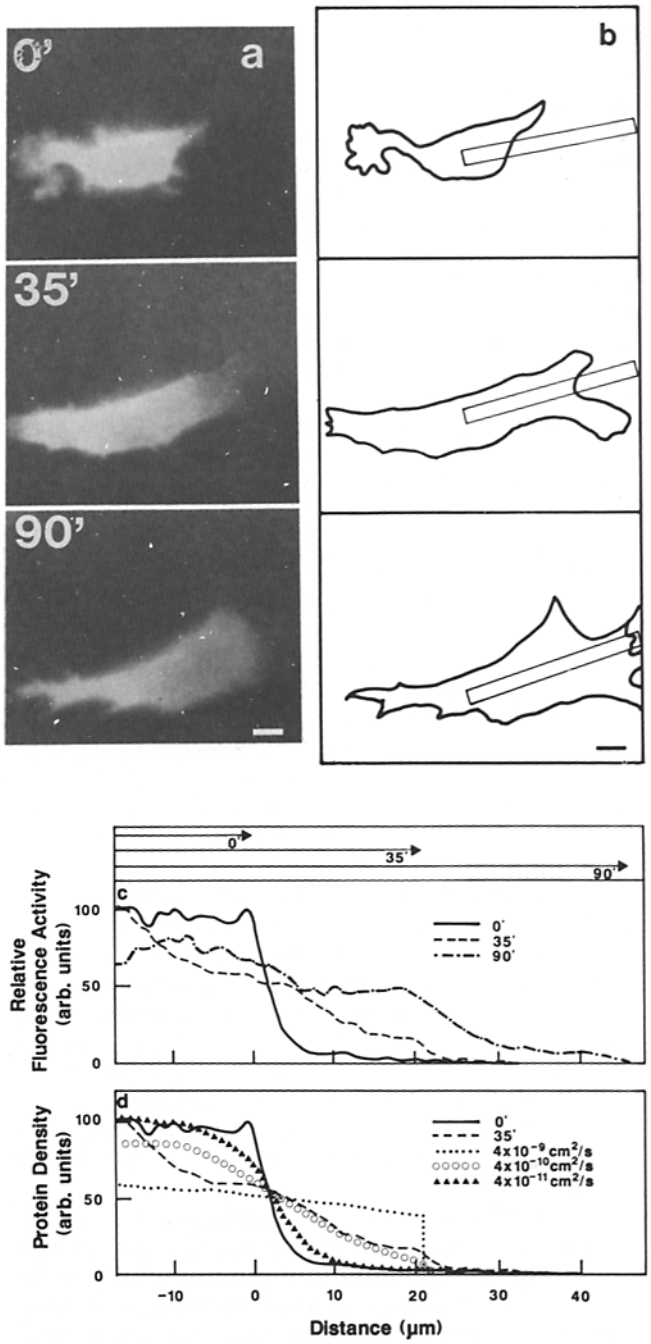

Figure 5. Redistribution of GP80 in spreading cells. As in Fig. 4, prechilled cells were labeled with R-anti-GP80 (95 μg/ml) and warmed to 37°C at time zero. The left column (*a*) shows the fluorescence images taken at 0, 35, and 90 min. The right column (*b*) shows the corresponding morphology of the cells. The boxes indicate the rectangular areas where the mean intensity profiles (*c*) were obtained. Bars in *a* and *b* indicate 10 μm. Panel *c* gives the mean intensity profiles of relative fluorecence intensity obtained by averaging individual profiles from the rectangular areas shown in *b*. The arrows at the top indicate the positions of the cell's leading edge. Panel *d* shows the theoretical predictions of GP80 distribution at 35′ when the distribution at time zero relaxed due to pure lateral diffusion. The calculation was carried out by computer simulation for various diffusion coefficients. The leading edge was assumed to advance at a constant rate of 0.6 μm/min. Reasonable agreement with the experimental result was obtained by taking $D = 4 \times 10^{-10}$ cm^2/s.

(Fig. 5 *a*). It is clearly noticeable that some fluorescence labeling moved into new leading edge area while diminishing somewhat in the preexisting area. These observations were quantitated by taking cross-sections of the fluorescence distribution along the cell axis (Fig. 5 *b*). Fig. 5 *c* shows these fluorescence profiles with respect to the leading edge (arrowtip in top panel) at the various times (0′, 35′, and 90′). This figure shows that the labeled GP80 was transported gradually into the newly extended area (to the right) as the extension continued. The ability of lateral diffusion to account for this transport was tested by comparing these experimental profiles with those expected, as simulated by computer, if the transport into the newly extended edge was caused by one-dimensional diffusion (Fig. 5 *d*). For these simulations, the leading edge was assumed to advance at a constant rate (0.6 μm/min) and the calculation was performed for three different diffusion coefficients (4×10^{-9}, 4×10^{-10}, 4×10^{-11} cm^2/s). It is seen that $D = 4 \times 10^{-10}$ cm^2/s comes closest to matching the experimental profile after 35 min.[2] It should be noted that 3.2×10^{-10} cm^2/s has been obtained as the diffusion coefficient for the GP80-mAb complex at 37°C by fluorescence recovery after photobleaching (Jacobson et al., 1984*a*). Qualitatively almost all the gradient relaxation processes were similar to the case shown in Fig. 5 in that the boundary between fluorescent and nonfluorescent zones was stationary and gradually eroded with time. In many cases, however, it was difficult to extract diffusion coefficients from the fluorescence profiles, because accompanying changes in cell shape added or subtracted intensity to or from the experimental profiles, respectively. Such profiles were difficult to fit to the calculated profiles which were assumed to change solely due to the effects of lateral diffusion.

About 40–60 min after warming cells, at which time the spread area had reached its maximum, most of the leading edges halted further extension and started to retract. The remaining edges (in most cases only one edge) continued to extend. The cell in Fig. 5 is a typical example; while the edge at the right continued to extend, the edge at the left turned into a trailing edge. The morphology of the retracting edges changed drastically from a round smooth shape to a spikelike shape, finally evolving into a morphology typical of trailing edges. Several retracting edges could be observed to merge into one trailing edge. The fluorescence distribution underwent characteristic changes accompanying these morphological alterations. Before retraction, lamellae were nearly devoid of fluorescence. As a lamella ceased or slowed extension, very gradual erosion of the gradient occurred. Then when retraction continued, the relative fluorescence intensity increased gradually at the retracting edges. As the cell morphology approached the typical morphology of locomoting cells, the "steady state" fluorescence gradient from leading edge to trailing edge became established as seen in the time series in Fig. 2.

2. A referee has pointed out that diffusion within a sector bounded by reflecting radii and proceeding from a point source placed at the vertex of the sector reaches equilibrium more rapidly than if one-dimensional diffusion along a radius is considered. Considering that such a model is an appropriate approximation to the cell shape and boundary condition, it predicts that the diffusion coefficient we calculate from one-dimensional gradient relaxation is actually an upper limit.

Distribution of Newly Appearing Anti-GP80 Binding Sites

Because the normal staining for immunofluorescence is a pulse labeling procedure, GP80 inserted after labeling would not be detected. Thus, the fluorescence distribution might not represent total GP80 distribution. To examine this possibility, cells were labeled with R-anti-GP80 initially and at a later time with F-anti-GP80. The distribution of fluorescence intensity was measured quantitatively by DFM as described in Materials and Methods. When F-anti-GP80 was applied immediately after staining with 100 μg/ml of R-anti-GP80 very little fluorescein staining was detected, indicating this antibody concentration blocked almost all the F-anti-GP80 binding sites on the cell surface (Fig. 6, *a* and *b*). The relative fluorescence intensity of this stain was 6% of the control in which cells were stained only with F-anti-GP80. When C3H/10T1/2 cells stained with R-anti-GP80 were incubated at 37°C for 1 h and then stained with F-anti-GP80, more fluorescein staining was observed (Fig. 6, *c* and *d*). The relative intensity of the fluorescence staining was 29% of the control. However, the fluorescein distribution was very similar to the rhodamine distribution. These new anti-GP80 binding sites are either newly synthesized and inserted GP80, recycled GP80, or existing surface GP80 from which the rhodamine antibody dissociated during the 1 h incubation. The third possibility is more likely for several reasons. When the same experiment was performed in the presence of 1 mM KCN to inhibit metabolism and depress recycling we found a nearly equivalent amount of F-anti-GP80 bound to the cell surface after a 60-min incubation at 37°C (data not shown). In addition, permeabilized fixed cell indirect immunofluorescence demonstrated that the internal pool size of GP80 was extremely small (data not shown). Finally, the turnover rate of GP80 is in excess of 48 h, indicating that only a small amount of GP80 is synthesized within 1 h.

Comparison of Experimental Results to Models Steady State Distribution

As will be argued in Discussion, the evidence indicates that the redistribution of GP80 is caused by lateral motions of the protein within the plane of the membrane. The cell locomotion models described in the Introduction predict the development of gradients via lateral movements of proteins constrained to the plane of the membrane. We attempted to compare quanitatively the experimental results with the numerical predictions of models and to evaluate whether the models may be able to serve as a semiquantitative explanation of the results. The theoretical models were reduced to one dimension and assume that locomotion continues at constant speed and direction. As a result, they represent only a very rough approximation in view of the complex morphology and discontinuous locomotory behavior of cells. The models assumed a 50-μm-long rectangular cell shape which contained a constant number of membrane protein molecules, and only molecular motions along the long axis (the axis parallel to cell locomotion) were considered. This simplification means that the long axis selected is assumed to be far enough from the lateral cell edges so that movements of GP80 along the axis perpendicular to the long axis will not significantly affect the gradient shape. A diffusion coefficient

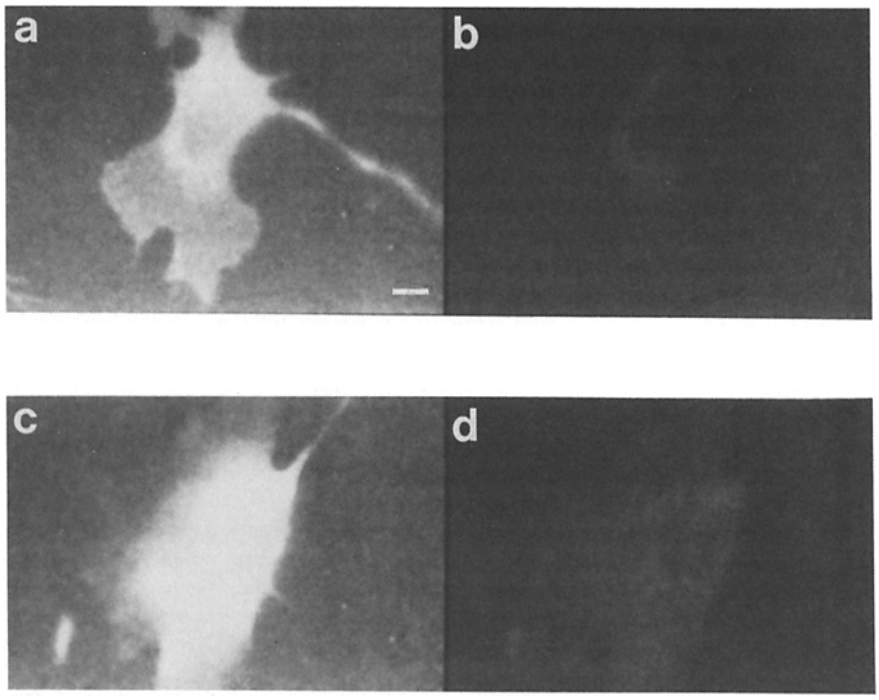

Figure 6. Distribution of newly appearing anti-GP80 binding sites. (*a* and *b*) Blocking control. Prechilled cells were first stained with 100 μg/ml of R-anti-GP80 and then immediately stained with 100 μg/ml F-anti-GP80. (*a*) The distribution of rhodamine labeling. (*b*) The distribution of fluorescein labeling. (*c* and *d*) Distribution of newly appearing anti-GP80 binding sites. Prechilled cells were first stained with R-anti-GP80, incubated at 37°C for 1 h, and then stained with F-anti-GP80. (*c*) The distribution of rhodamine labeling. (*d*) The distribution of fluorescein labeling. Bar, 10 μm.

at 37°C for GP80 of 3.2 × 10^{-10} cm^2/s was used (Jacobson et al., 1984*a*) unless otherwise noted. Some model predictions were obtained by analytical calculation but in most cases by computer simulation (see Materials and Methods for the details).

The two models tested in the present paper include assumption of a directional lipid flow. Whether membrane proteins are carried along with lipid flow or not depends on how free the proteins are in the plasma membrane. As described in Introduction, to explain the low diffusion coefficient of GP80, Jacobson et al. (1984*b*) postulated that individual GP80 molecules were transiently anchored to certain peripheral structures a very high percentage (>95%) of the time. Based on this model it is reasonable to suppose that the transiently anchored proteins are not carried along by the directional lipid flow; but rather are protected from the flow. The RIS model was developed by combining this view of transiently anchored protein and the retraction-induced spreading observation. On the other hand, the original RLF model is based on the view that membrane proteins are freely mobile in the plane of the membrane and thus that all protein molecules are equally subject to the lipid flow. Thus the two models are based on two different views of membrane protein mobility. However, to more completely test the potential of these models, we ran the simulations assuming that GP80 was either freely mobile or transiently tethered for both models. The ability of the models to account for features of the experimental data is summarized in Table I.

Retrograde Lipid Flow (RLF) Model. This model (see Fig. 7 *a* and Introduction), proposed in its most quantitative form by Bretscher (1981, 1984), assumes front-to-rear flow of lipid and freely mobile membrane proteins, all equally subject to the flow. Fig. 7 *b* schematically depicts the computer simulation of this model. The steady state distribution was calculated under various assumptions. If the lipid in the plasma membrane flows rearward at a constant velocity, the gradated surface concentration of a nonrecycling protein, C(x), is given by (Bretscher, 1981):

$$C(x) = C_o \exp(-V_f x/D) \quad (1)$$

where V_f is the lipid flow rate, D is the lateral diffusion coefficient of the protein, x is the distance from the trailing edge of the cell and C_o is the surface concentration at x = o. We assumed that the velocity of the particles, 0.5 μm/min (Abercrombie et al., 1970*c*), was equal to the lipid flow rate relative to the substrate. Similar particle velocities on C3H/10T1/2 cells were obtained in our measurements (Holifield et al., unpublished information). The gradient predicted for this situation was obtained analytically (Eq. 1) and also by computer simulation (Fig. 8 *a*). The simulation matched the analytical prediction, providing a check on the simulation program. However, when this prediction was compared with the experimental result (the mean gradient of Fig. 3) poor agreement was achieved (compare theoretical [solid] and experimental [broken] curves in Fig. 8 *a*). In the simulation, ~77% of the total protein was concentrated in the rearmost 10% of the cell dimension, whereas experimentally only 17% of the protein population was in this same 10% region.

Fig. 8 *b* represents a modified model, with endocytosis occuring at equal rates over the entire cell surface resulting in a rearward flow velocity which decreases from the front to the rear (Bretscher, 1984).[3] In Fig. 8 *b* the flow velocity

3. The steady state distribution for this model can be obtained analytically. We assumed a one-dimensional cell, length L, in which the retrograde flow decreased linearly from front to rear according to: $V_f(x) = [xVo/L]$, where $V_f(x)$ is the flow velocity at any point x and Vo is the maximum flow velocity at x = 0, the front of the cell. The net flux, J, at any point x is given by the sum of a diffusive term and a flow term: $J(x) = -D(dC/dx) + VoxC/L$, where C is the concentration at any given point x and D is the diffusion coefficient. In the steady state, $J(x) = 0$ and the preceding equation can be integrated to yield: $C(x) = Co \exp(-Vx^2/2DL)$.

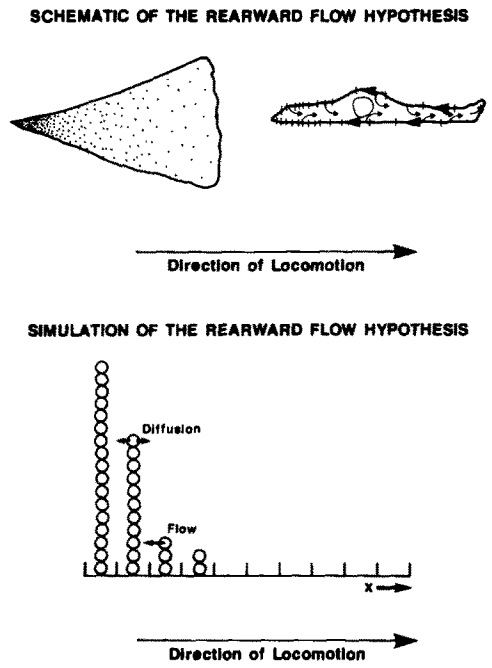

Figure 7. Schematic diagram of the rearward flow hypothesis and its simulation. (*a*) The model postulates the recycling of membrane lipids. Membrane lipids with some recycling proteins are internalized as endocytosis occurs over the cell surface; recycled lipids are translocated to the front of the cell and inserted to form a new leading edge. On the cell surface lipids flow rearward (←) and membrane proteins tend to be carried with the flow, resulting in the formation of surface concentration gradient. The gradient is steeper when the flow velocity is faster or when the diffusion coefficient is smaller. (*b*) Scheme of one-dimensional simulation. A cell was represented by a linear array of bins, and a number of particles representing membrane proteins were distributed in each of the bins. Actual simulation was carried out with 100 bins and 10,000 particles. The particles were transferred from bin to bin under the following rules. Diffusion operation: each particle is transferred randomly to one of the two adjacent bins. Flow operation: each particle is transferred to the adjacent bin to the left to represent retrograde flow. The diffusional operation was repeated successively with intermittent insertion of the flow operation to simulate realistic flow rates. For further details, see Materials and Methods.

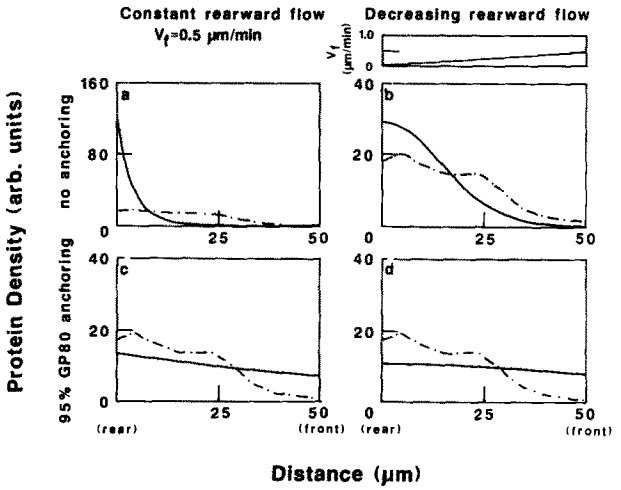

Figure 8. Predicted steady state distributions of membrane proteins based on the retrograde lipid flow model. The figures show the membrane protein, density from the front (the right end) to the rear (the left end) along the 50-μm-long cell axis. Broken lines indicate the mean steady state distribution obtained experimentally as transferred from Fig. 3. Solid lines give the simulation results. The area under the distributions represents the total amount of the membrane protein and is arranged to be identical for each plot. The flow velocity (V_f) was defined as relative to the substratum. In all cases, a D of 3.2 × 10^{-10} cm^2/s was assumed. (*a* and *c*) V_f was assumed to be constant from the front to the rear end (0.5 μm/min). (*b* and *d*) V_f was assumed to decrease linearly from the front end (0.5 μm/min) to the rear end (0 μm/min) as indicated in the panel at the top of the figure. In *a* and *b* no anchoring of GP80 was assumed, whereas in *c* and *d* transient anchoring of 95% of the protein population was assumed.

decreases linearly from 0.5 μm/min at the front to zero at the rear end. This model yields a much shallower steady state distribution, giving a better match of theory to experiment.

Next, in a departure from the original RLF model, transient anchorage of the proteins was assumed to occur. When the retrograde lipid flow rate was constant (0.5 μm/min), the resulting distribution was shallow (Fig. 8 *c*), resulting in better agreement of model and experiment at the rear of the cell. However, the marked depletion of protein at the leading edge was not predicted. When the flow rate was decreased linearly from the front to the rear, the distribution becomes almost uniform (Fig. 8 *d*) and displays none of the features of the experimental gradient.

Finally, it should be noted that if the diffusion coefficient for GP80 was much greater (i.e., D = 10^{-8} cm^2/s) no appreciable gradient is obtained (Bretscher, 1981; simulation not shown), as diffusion overwhelms the flow.

Retraction-induced Spreading (RIS) Model. This model (see Introduction) is depicted in Fig. 9 *a*. Fig. 9 *b* shows a schematic of the simulation for the RIS model. Retraction was assumed to occur as a uniform shortening of the cell's rear half. The length (area) gained by this shortening is deposited at the front of the cell to simulate retraction-induced spreading, and both the retraction and deposition processes were assumed to proceed at a rate of 0.5 μm/min. The forward membrane flow rate relative to the substratum was increased from 0 μm/min at the rear end to 0.5 μm/min at the midpoint of one cell and was assumed to be constant at 0.5 μm/min from this point to the front edge. The speed of extension in the front half of the cell was taken from our measurement of leading edge extension. The graded flow velocity in the rear half was derived from the assumption of uniform shortening. We further assumed that 95% of the membrane protein was transiently anchored in accord with the model proposed by Jacobson et al. (1984*a*).

Comparisons of the model to experiment (Fig. 3) are given in Fig. 10. The resultant curve (Fig. 10 *a*) is seen to be somewhat steeper than the mean experimental gradient experimental data, but in reasonable agreement with the steepest gradients of Fig. 3, presumably associated with the most actively moving cells. (Compare also prediction to gradients shown for one cell in Fig. 2 *d*). When no anchoring was assumed (Fig. 10 *b*), no gradient was obtained as the membrane proteins were carried along with the forward flow.

Formation and Erosion of the Boundary

Experimentally we observed that newly extended lamellae have very little fluorescence, resulting in the formation of a pronounced fluorescence boundary between the edge and the

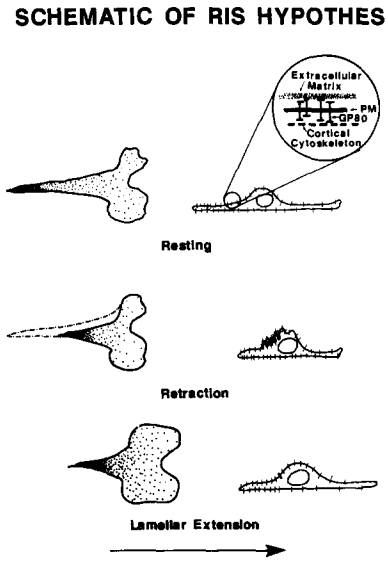

Figure 9. (*a*) Schematic diagram of RIS hypothesis. Tail retraction produces a membrane reservoir, in the form of dorsal folds (*a*, *middle*). As lamellar extension ensues, presumably driven by cytoskeletal modification, membrane flows forward as these folds are stretched out to provide the surface for the new leading edge (*a*, *bottom*). Second, GP80 is assumed to be transiently anchored to structures peripheral to the membrane (*a*, *top*), and as the lipids and unanchored protein flow forward, GP80 and any other transiently anchored proteins are, in effect, conveyed toward the rear producing an accumulation of protein in this region. Because the anchoring is not permanent, the resultant slow protein diffusion erodes this accumulation to some extent. (*b*) Scheme of the simplified model was used for the computer simulation of the RIS model. The model consists of four operations. First tail retraction was modeled by the shortening of the rear half of the cell or a portion thereof. The bin number in the rear half was reduced from 51 to 50 and the particles present in those bins were redistributed in the reduced number of bins in proportion to the original distribution. Second, to simulate leading edge extension the one empty bin created in the first step was added to the front end. Third, to simulate the forward flow, particles were moved to the next bin in the downstream side (to the right). Finally, each particle was randomly transferred to one of the two adjacent bins to simulate random diffusion. (For further details, see Materials and Methods).

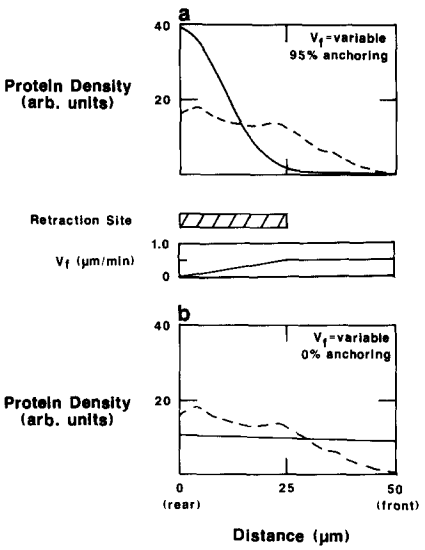

Figure 10. Predicted steady state distributions for RIS model. The broken lines indicate the mean steady state distribution obtained experimentally (see Fig. 3). The solid line give the simulation results. The steady state distributions for RIS model were calculated by computer simulation as depicted in Fig. 9 *b*. *D* was assumed to be 3.2×10^{-10} cm²/s for GP80. The retraction site on the cell surface (hatched region at middle of figure) was compressed uniformly at a constant rate (0.5 μm/min). Membrane was assumed to flow forward, its velocity (V_f) increasing from 0 at the rear end to 0.5 μm/min at the cell midpoint; from the midpoint to the leading edge V_f was constant at 0.5 μm/mm. (*a*) 95% of the membrane proteins were assumed to be transiently anchored. (*b*) All proteins were assumed to be mobile.

perinuclear region (see Figs. 4 and 5). Any subsequent erosion of this boundary appeared to be accounted for by simple lateral diffusion of GP80 (Fig. 5) and the midpoint of the boundary never appeared to move rearward relative to the substratum. We examined by computer simulation the ability of each of the models discussed above to account for this phenomenon. It was assumed that upon warming, a prechilled cell extended a new leading edge and formed a boundary (Fig. 11 *a*) subject to the following conditions. (*a*) Initially, a cell had a uniform GP80 distribution over its surface described by a constant protein concentration. (*b*) The cell started to extend a new leading edge at time zero with a constant velocity of 0.5 μm/min. (*c*) The lateral diffusion coefficient of GP80 was 3.2×10^{-10} cm²/s.

RLF Model. As the leading edge is extended, it was assumed that the lipid flows from the tip of the leading edge to the end of the cell. We defined the flow velocity relative to the substratum, not to the extending leading edge. In Fig. 11 *b*, membrane flows rearward with a constant velocity (0.5 μm/min) yielding massive accumulation of GP80 at the rear of the cell and retrograde movement of the boundary which has been simulataneously eroded by diffusion. In Fig. 11 *c*, the velocity of retrograde lipid flow was assumed to decrease from the front to the rear. Although much less accumulation occurs at the very rear of the cell, the boundary still moves ~12 μm rearward during the first 40 min. These simulations make two important points. First, significant (10–20 μm) retrograde movement of the boundary can be expected according to the RLF model over the course of an hour. Second, the retrograde flow should prevent appreciable fluorescence from entering new lamellae via diffusion, a prediction in clear contradiction with experiment. (See, for example,

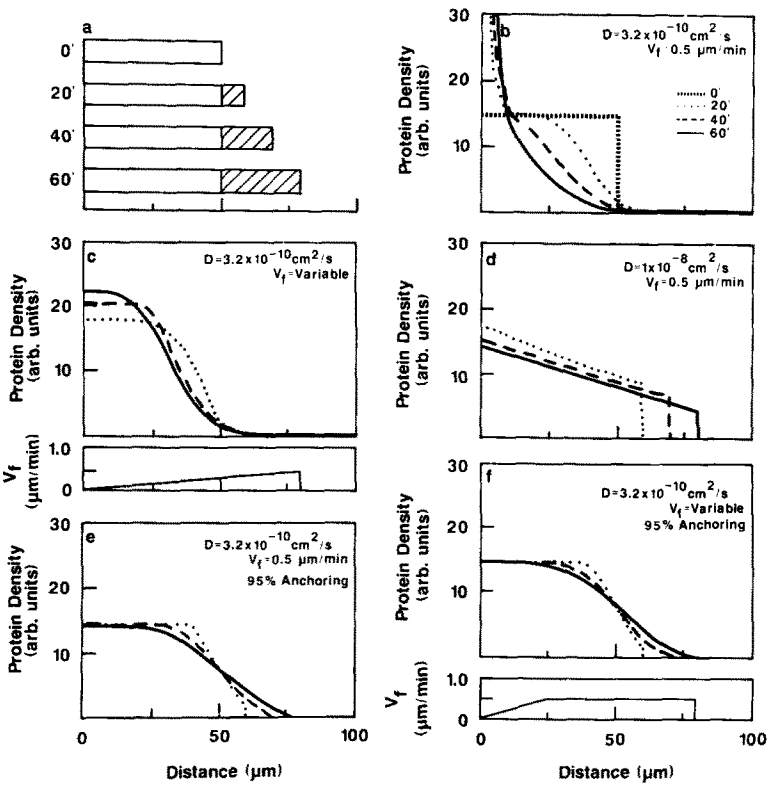

Figure 11. Predicted GP80 distribution changes upon the extension of new leading edges according to the RLF (*b–e*) and the RIS (*f*) model. (*a*) The model assumes a 50-μm-long cell in which a membrane protein is initially distributed uniformly over the cell surface. At time zero, the cell starts extending, a new leading edge in one direction at the rate of 0.5 μm/min (indicated by the hatched region). The subsequent redistribution at 20 min (. . . .), 40 min (- - - -), and 60 min (———) was calculated by computer simulation. The flow velocity (V_f) of the retrograde lipid flow or forward lipid flow, depending on the model employed, was defined relative to a fixed point on the substratum. A diffusion coefficient of 3.2×10^{-10} cm²/s was used except in *d*. (*b*) The retrograde lipid flow velocity was assumed to be constant (0.5 μm/min) and the initial distribution at time zero is indicated by (mmm). (*c*) The retrograde flow velocity was assumed to decrease from the front to the rear end of the cell as shown in the panel at the bottom of the figure. (*d*) 1×10^{-8} cm²/s was used for *D* and the retrograde lipid flow velocity was assumed to be constant (0.5 μm/min). (*e*) A constant retrograde flow velocity (0.5 μm/min) was assumed but 95% of the proteins were assumed to be transiently anchored and not subject to the flow. (*f*) Predicted GP80 distribution changes upon the extension of new leading edges according to the RIS model. Leading edge extension and the accompanying forward flow were considered but no tail retraction was assumed. In the simulation, 95% protein anchoring and a variable forward flow velocity was assumed as shown in the panel at the bottom of the figure.

leftmost lamellae in Fig. 4, 45 and 60 min right micrographs.)

Fig. 11 *d* shows the case where the diffusion coefficient is assumed to be 1×10^{-8} cm²/s and the membrane flows rearward with a constant velocity of 0.5 μm/min; lateral diffusion dominates the flow effect and the new leading edge is occupied by GP80 almost instantaneously as the edge extends in contradiction with the experimental result. Fig. 11 *e* shows the case in which the flow rate is constant and 95% of the GP80 was transiently anchored. Because most of the GP80 is "protected" from the flow, it has little effect and the result approximates that when only lateral diffusion is operative. In this situation little boundary movement occurs. A very similar result was obtained when the flow rate was assumed to decrease going toward the trailing edge (data not shown).

RIS Model. In evaluating the ability of the RIS model to account for the lack of boundary movement, it was assumed that a prechilled cell had a membrane reservoir initially and upon temperature increase the membrane flowed forward to form a new leading lamella. As above GP80 was assumed to diffuse with $D = 3.2 \times 10^{-10}$ cm²/s but with 95% of the proteins transiently anchored leaving only 5% subject to this forward flow at a given time. As shown in Fig. 11 *f*, the flow had little effect so the boundary midpoint exhibited no movement. This prediction of a static boundary agrees with experiment. If the transient anchoring is not assumed, GP80 flows forward as the leading edge extends and no boundary is expected to be formed (data not shown).

Discussion

Our objective in this study was to monitor the dynamics of the redistribution of a major plasma membrane protein, GP80, on motile murine fibroblasts. The combination of low light level digitized fluorescence microscopy and direct immunofluorescence utilizing mAb labeling made it possible to image the distribution changes of a single class of membrane proteins in individual cells during the process of cell locomotion. This method provides spatially resolved photometric data so that the lateral distributions are expressed in quantitative terms (Kapitza et al., 1985; DiGuiseppi et al., 1985; Arndt-Jovin et al., 1985). Providing the exposure of the cells to the excitation light was minimized, cell locomotion appeared not to be appreciably affected by this measurement.

The major findings of this study are: (*a*) labeled GP80 exhibited a distribution that was coupled with cell locomotion; motile cells exhibited a pronounced gradient, increasing from the front to the rear, whereas the fluorescence distribution in stationary cells was nearly uniform. This result confirmed earlier studies using fixed cell indirect immunofluorescence photography and spot photometry (Jacobson et al., 1984*b*). (*b*) The GP80-mAb gradient existed, qualitatively, as a "steady state" in continuously motile cells. (*c*) The newly extended leading edges were almost devoid of fluorescence labeling. This was strikingly demonstrated after warming prechilled cells where the extension of fluorescence-free leading edges caused a pronounced boundary between fluorescent and nonfluorescent zones. As the leading

edge extension continued, the boundary gradually blurred; this boundary erosion occurred in a manner expected due to the lateral diffusion of GP80 in the plane of the plasma membrane.

Several lines of evidence suggest that the fluorescence redistributions observed above are caused primarily by the lateral motions of GP80 in the plasma membrane and not via intracellular membrane traffic. First, the turnover rates of GP80 appears to be slow. Our previous study showed that the fluorescent labeled GP80 remained at the cell surface for long periods (>100 h), with no detectable internalization (Jacobson, 1984*b*). Furthermore, a recent measurement of the turnover time for GP80 revealed that it was in excess of 48 h (deSousa and August, unpublished). Presumably the amount of newly synthesized GP80 inserted into the plasma membrane during our experiment would be negligible (<4%) and this is supported by the fact that after trypsinization it takes 24 h or more to regain appreciable anti-GP80 binding as judged by the intensity of fluorescence staining (Jacobson et al., unpublished). Second, it is also likely that the recycling rate of GP80 is small. Earlier experiments failed to detect the internalization of GP80 antibody complexes, the first step in recycling. Furthermore, permeabilized fixed cell indirect immunofluorescence indicated a very small pool of internal GP80. Indeed, Bretscher et al. (1980), found that GP80 (the H63 antigen in his notation) failed to appear in coated pits, suggesting that it is not a rapidly recycling protein. However, Murphy et al. (1983) did not confirm this result.

The GP80-mAb gradient was found to exist in a "steady state." In the case of a pulse-labeling measurement such as this, one must ascertain whether the fluorescence distribution represents the total surface distribution of the protein, because insertion of newly synthesized protein after labeling or dissociation of the label from the antigen could cause the actual GP80 distribution to differ from that reported by fluorescence staining. The amount of newly inserted GP80 appears to be negligible during the experimental period as described above. While some dissociation of antibody may occur (Jacobson et al., 1984*a*) it should occur at the same rate over the cell surface and therefore should not distort the gradient shape.

While GP80 displays a gradated distribution in some motile cells (Ishihara et al., 1988) as determined by indirect immunofluorescence of prefixed cells, we showed previously (Jacobson et al., 1984*b*) that the gradient of GP80-mAb complex became steeper during a 12-h period after applying the antibody. We have since determined that the steeper gradient is established within 1 h (data not shown). In the present study GP80 was labeled with fluorescent monoclonal anti-GP80 and then cells were allowed to locomote for periods up to or greater than 1 h. Consequently, the steady-state gradients measured and analyzed over these time periods are steeper than the endogeneous gradated GP80 distribution.

Polarized distributions of membrane proteins are common in locomoting cells under conditions where the proteins are extensively crosslinked by multivalent ligands; this situation is known as the "capping" phenomenon. Although the occurrence of the gradient described in this report has similarities with capping phenomenon, it should be noted that differences exist. First, capping is viewed to be induced by the application of multivalent antibodies which aggregate the initially diffusely distributed proteins (De Petris and Raff, 1973). In contrast, after labeling GP80 with fluorescent monoclonal anti-GP80, the distribution remains diffuse for >100 h (Jacobson et al., 1984*b*) and, as this report demonstrates, the gradient is maintained in an approximate steady state. Visible aggregation of labeled GP80 will occur only upon addition of secondary antibodies that crosslink the monoclonal anti-GP80; aggregation occurs within minutes and capping is complete in 30–60 min (Jacobson et al., 1984*b*). Explanations of the mechanism of capping are controversial and include retrograde lipid flow and cortical cytoskeletal contraction. In this report we have focused only on the contributions of forward and rearward membrane flows to the establishment and maintenance of the GP80 gradient. Possible involvement of cortical cytoskeletal contraction cannot be ruled out at this time, but consideration of such involvement must await an experimental basis.

GP80 appears to function as a cell adhesion molecule (August et al., personal communication). It is possible, therefore, that a cell may find it advantageous to have some of the molecules responsible for cell surface "stickiness" to the extracellular environment partitioned toward the rear during locomotion. Unencumbered by excessive extracellular matrix, the leading edge may have greater flexibility in sampling potential adhesion sites. Furthermore, having molecules such as GP80 preferentially toward the rear may provide an essential link between the tension-developing apparatus within the cytoplasm and the substrate. Such tension is apparently a prerequisite for the tail detachment and retraction phase.

A few observations have been reported on gradients of uncrosslinked membrane proteins. Ryan et al. (1974) did observe a gradient of fluorescence labeling on polymorphonuclear leucocytes. Braun et al. (1978) reported that some membrane proteins were concentrated in one end of pre-fixed polarized lymphocytes.

There are also observations in which membrane proteins did not exhibit a gradated distribution in locomoting cells. Middleton (1979) found that the Thy-1 antigen was distributed uniformly over the surface of locomoting fibroblasts, including the newly extended leading edge area. We observed a similar uniform distribution for Thy-1 in locomoting C3H/10T1/2 cells (Ishihara et al., 1988). This result may be related to the very rapid lateral diffusion of Thy-1 (Ishihara et al., 1987), which counteracts gradient formation mechanisms. Middleton (1979), based on his observation that the prelabeled Thy-1 also existed in newly extended lamellae, argued that there was no new membrane insertion in the leading edges. Our result, contrary to that of Middleton, showed that very little GP80 was detected in newly extended leading edge area. However, we think this result can be interpreted in at least two ways, as shall be discussed, and is not necessarily proof for membrane insertion.

Some membrane proteins are preferentially localized toward the leading edge of motile cells. These proteins include receptors for transferrin (Bretscher, 1983; Ekblom et al., 1983; Hopkins, 1985), receptors for low density lipoproteins (Bretscher, 1983), and the F_c receptors on polarized PMNs (Walter et al., 1980). Unlike GP80, these proteins are known to recycle. In addition, a recent study (Petty and Francis, 1986) showed that histamine receptors were localized in leading edges of locomoting PMNs.

Comparison of the Results with Cell Locomotion Models

Our results suggested that the observed redistribution was due to the lateral motion of GP80 in the plasma membrane with no appreciable contribution from either endocytosis, cytoplasmic transport, and reinsertion of GP80 or new synthesis of the glycoprotein. This means that the two models described briefly in the Introduction are applicable and can be evaluated. Qualitatively, both models predict the absence of GP80 in the extended leading edge and that the gradated GP80 distribution is coupled with cell locomotion.

We attempted a quantitative evaluation of the two models. The distributions predicted by the model were calculated by computer simulation and these results were compared with the experimental distributions both at steady state and after warming chilled cells to activate lamellar extension. The summary of the comparison is shown in Table I. The models we have employed were greatly simplified for computational tractibility and thus ignored several significant factors in cell locomotion which could affect the GP80 distributions. These factors include (*a*) the reduction to one dimension which represents a gross approximation considering the complex cell morphologies observed, and (*b*) the fact that both tail retraction and leading edge extension are not continuous activities but occur in a discontinuous manner with variable rates. Thus, the fact that locally steep gradients of short duration may be produced by rapid tail retraction or very rapid spreading at the leading edge is not described by these models in their current form.

Retrograde Lipid Flow Model. The steady state distribution curve is determined by two parameters: the lipid flow velocity and the lateral diffusion coefficient of GP80. We employed a value of 3.2×10^{-10} cm^2/s for the diffusion coefficient, consistent with the results obtained at 37°C by fluorescence recovery after photobleaching (Jacobson et al., 1984*a*). The flow velocity, assuming that retrograde particle movement reflects the lipid flow, was taken to be 0.5 μm/min as measured in chicken embryo fibroblasts (Ambercrombie et al., 1970*c*). This value is also consistent with results obtained for particle motion on C3H/10T1/2 cells (Holifield et al., unpublished information).

If a constant retrograde flow (0.5 μm/min) acts on all GP80 molecules as assumed in the original model, the simulated steady state distribution was much steeper than the experimental profile. If the flow was assumed to decrease linearly from 0.5 μm/min at the front to zero at the rear, the steady state distribution was similar to the experiment result (Fig. 8 *b*). However, in both cases the fluorescent boundary existing in spreading cells is expected to move rearward (Fig. 11, *b* and *c*), whereas experiments showed that this boundary was nearly stationary with respect to the substrate when prechilled cells spread.

It is also necessary to consider the tenability of the RLF model in terms of current knowledge about the mobility of membrane proteins. Bretscher has argued that membrane proteins should have lateral diffusion coefficients in the range of 10^{-8} cm^2/s and that the lower values often obtained in photobleaching measurements may be artifactual (Bretscher, 1982). In fact, this study indirectly supports the lower values obtained for GP80 (Jacobson et al., 1984*a*) by the FRAP technique. First, the kinetics of GP80 redistribution in spreading cells (Fig. 5) are consistent with much lower lateral diffusion coefficients ($D = \sim 4 \times 10^{-10}$ cm^2/s). Second, none of the features of the experimental data can be ex-

Table I. Ability of Models to Account for Experimental Data

	Feature of experimental data	
Model	Steady state gradient	Lack of boundary movement during spreading
RLF		
Unanchored proteins		
Constant flow	Predicts much more accumulation in trailing edge than exists (Fig. 8 *a*)	Predicts rearward boundary movement (Fig. 11 *b*)
Flow decreasing toward rear	Correctly predicts depletion in leading edge, accumulation in trailing edge in reasonable agreement with experiment (Fig. 8 *b*)	Predicts rearward boundary movement (Fig. 11 *c*)
Constant (or decreasing) flow with proteins which have much greater D ($=10^{-8}$ cm^2/s)	No appreciable gradient predicted (not shown)	No boundary predicted as leading edge is quickly occupied by GP80 (Fig. 11 *d*)
Transiently anchored proteins		
Constant flow	Predicts much less depletion in leading edge than exists (Fig. 8 *b*)	Correctly predicts lack of boundary movements (Fig. 11 *e*)
Flow decreasing toward rear	Predicts much less depletion in leading edge and less accumulation in trailing edge than exists (Fig. 8 *d*)	Correctly predicts lack of boundary movement (not shown)
RIS		
With transiently anchored proteins	Correctly predicts depletion in leading edge, accumulation in trailing edge in reasonable agreements with higher gradients in Fig. 3 (Fig. 10 *a*)	Correctly predicts lack of movement (Fig. 11 *f*)
With unanchored proteins	Predicts no gradient should exist (Fig. 10 *b*)	No boundary expected (not shown)

plained by either model if the lateral diffusion coefficient of GP80 was as high as 10^{-8} cm^2/s. Further, the RLF model requires that the flow act on all GP80 molecules equally. This is tantamount to saying that all GP80 molecules diffuse as free particles in the bilayer medium with a diffusion coefficient of $\sim 3 \times 10^{-10}$ cm^2/s. Yet proteins reconstituted into artificial bilayers exhibit lateral diffusion coefficients nearly 100 times larger with little dependence on diffusant size (Vaz et al., 1984). And crowding in even the most densely packed organelle produces at most an order of magnitude reduction in protein diffusion coefficients (Vaz et al., 1984). Therefore, the reduced apparent diffusion coefficients which have been measured for many membrane proteins, such as GP80, are most likely due, at least in part, to transient interactions with structures peripheral to the membrane. If this condition is included in the RLF simulation, GP80 is "protected" from the retrograde flow. Whereas this modification correctly predicts the lack of rearward boundary movement in spreading cells, it yields a neglible steady state gradient which is inconsistent with experiment. Thus, neither the original nor the modified RLF model can predict all features of the experimental data.

RIS Model. The RIS model can be simulated using the D for GP80, the percentage of the GP80 population transiently anchored, the cell locomotion rate, and the site and dimension of the retraction region. Employing parameters drawn from measurement and observation, the simulated steady-state distributions approximated the experimental results. In addition, this model predicts the observation of a stationary but eroding boundary on spreading cells (Fig. 11 *f*). Thus, the RIS model is able to provide a better fit to the total body of experimental data than does the RLF model.

The RIS model, in its current form, does not address how recycling membrane proteins redistribute during locomotion. This issue remains to be studied further.

Conclusions

Two major activities involved in the locomotion of fibroblasts are the extension of leading edges and retraction of trailing edges. These two activities contribute to the establishment of the gradated fluorescence distribution whereas lateral diffusion of the glycoprotein-mAb complex tends to dissipate any gradients. Because GP80 is slowly internalized and its turnover rate is low, the insertion of newly synthesized or recycled GP80 into the plasma membrane, degradation of GP80, and the translocation of GP80 through the cytoplasm are probably not major factors contributing to the observed redistribution. We evaluated the ability of two models to account for the gradated distribution of GP80 in locomoting cells, the RLF model and the RIS hypothesis, recognizing that these two extreme models are an oversimplification of an exceedingly complex phenomenon and under certain circumstances a cell could conceivably employ either or both mechanisms (Trinkaus, 1985). Both models predict the steady state gradient of GP80 concentration in motile cells. However, the RLF model requires that GP80 freely diffuse with $D = \sim 3 \times 10^{-10}$ cm^2/s. This assumption seems unwarranted in light of our present knowledge about the lateral mobility of membrane proteins. Most likely, proteins exhibiting reduced diffusion coefficients do so because of interactions with structures peripheral to the membrane bilayer. It is these postulated interactions that are employed to produce the gradient in the RIS model. Furthermore, the RLF model fails to predict the observed lack of rearward boundary movement in spreading cells. On the other hand, the RIS model adequately accounts for this feature of the experimental data. In any case, the direction of the putative lipid flows remains to be established by direct experiment.

We thank Dr. Mark Bretscher for his thoughtful comments. We also thank Dr. Charles Hackenbrock, Chair, Dept. of Cell Biology and Anatomy, for his support and encouragement during the development of the DFM technology.

This work was supported by National Institutes of Health grants GM 29234 and GM31168, American Cancer Society Grant CD-181B, and American Heart Association Grant-in-Aid 83-1325.

References

Abercrombie, M., J. E. M. Heaysman, and S. M. Pergrum. 1970*a*. The locomotion of fibroblasts in culture. I. Movements of the leading edge. *Exp. Cell Res.* 59:393–398.

Abercrombie, M., J. E. M. Heaysman, and S. M. Pergrum. 1970*b*. The locomotion of fibroblasts in culture. II. "Ruffling." *Exp. Cell Res.* 60:437–444.

Abercrombie, M., J. E. M. Heaysman, and S. M. Pergrum. 1970*c*. The locomotion of fibroblasts in culture. III. Movements of particles on dorsal surface of the leading lamella. *Exp. Cell Res.* 62:389–398.

Arndt-Jovin, D. J., M. Robert-Nicoud, S. J. Kaufman, and T. M. Jovin. 1985. Fluorescence digital imaging microscopy in cell biology. *Science (Wash. DC).* 230:247–256.

Benson, D. M., J. Bryan, A. L. Plant, A. M. Gotto, Jr., and L. C. Smith. 1985. Digital imaging fluorescence microscopy: spatial heterogeneity of photobleaching rate constants in individual cells. *J. Cell Biol.* 100:1309–1323.

Berg, H. C. 1983. Random Walks in Biology. Princeton University Press, Princeton, N. J. 130–132.

Bergmann, J. E., A. Kupfer, and S. J. Singer. 1983. Membrane insertion at the leading edge of motile fibroblasts. *Proc. Natl. Acad. Sci. USA.* 80: 1367–1371.

Braun, J., K. Fujiwara, T. D. Pollard, and E. R. Unanue. 1978. Two distinct mechanisms for redistribution of lymphocyte surface macromolecules. I. Relationship to cytoplasmic myosin. *J. Cell Biol.* 79:409–418.

Bretscher, M. S. 1981. Surface uptake by fibroblasts and its consequences. *Cold Spring Harbor Symp. Quant. Biol.* 46:707–713.

Bretscher, M. S. 1982. Lateral diffusion in eukaryotic cell membranes. *Trends Biochem. Sci.* 5:6–7.

Bretscher, M. S. 1983. Distribution of receptors for transferrin and low density lipoprotein on the surface of giant Hera cells. *Proc. Natl. Acad. Sci. USA.* 80:454–458.

Bretscher, M. S. 1984. Endocytosis: relation to capping and cell locomotion. *Science (Wash. DC).* 224:681–686.

Bretscher, M. S., J. N. Thompson, and B. M. F. Pearse. 1980. Coated pits act as molecular filters. *Proc. Natl. Acad. Sci. USA.* 77:4156–4159.

Chen, W.-T. 1979. Induction of spreading during fibroblast movement. *J. Cell Biol.* 81:684–691.

Chen, W.-T. 1981*a*. Surface changes during retraction-induced spreading of fibroblasts. *J. Cell Sci.* 49:1–13.

Chen, W.-T. 1981*b*. Mechanism of retraction of the trailing edge during fibroblast movement. *J. Cell Biol.* 90:187–200.

Colombatti, A., E. N. Hughes, B. A. Taylor, and J. T. August. 1982. Gene for a major cell surface glycoprotein of mouse macrophages and other phagocytic cells is on chromosome 2. *Proc. Natl. Acad. Sci. USA.* 79:1926–1929.

Dembo, M., L. Tuckerman, and W. Goad. 1981. Motion of polymorphonuclear leukocytes: theory of receptor redistribution and the frictional force on a moving cell. *Cell Motility.* 1:205–235.

DePetris, S., and M. C. Raff. 1973. Fluidity of the plasma membrane and its implication for cell movement. *CIBA Found. Symp.* 14:27–55.

Derzko, Z., and K. Jacobson. 1980. Comparative lateral diffusion of fluorescent lipid analogs in phospholipid multibilayers. *Biochemistry.* 19:6050–6057.

DiGuiseppi, J., R. Inman, A. Ishihara, K. Jacobson, and B. Herman. 1985. Applications of digitized fluorescence microscopy to problems in cell biology. *Biotechniques.* 3:394–403.

Dunn, G. A. 1980. Mechanisms of fibroblast locomotions in cell adhesion and motility. The Third Symposium of the British Society for Cell Biology. A. S. G. Curtis and J. D. Pitts, editors. Cambridge University Press, Cambridge, England. 409–423.

Ekblom, P., I. Thesleff, V.-P. Lehto, and I. Virtanen. 1983. Distribution of the transferrin receptor in normal human fibroblasts and fibrosarcoma cells. *Int. J. Cancer.* 31:111–117.

Erickson, C. A., and J. P. Trinkaus. 1976. Microvilli and blebs as sources of reserve surface membrane during cell spreading. *Expl. Cell Res.* 99:375–384.

Harris, A. K., and G. Dunn. 1972. Centripetal transport of attached particles on both surfaces of moving fibroblasts. *Exp. Cell Res.* 73:519–523.

Hopkins, C. R. 1985. The appearance and internalization of transferrin receptors at the margins of spreading human tumor cells. *Cell.* 40:199–208.

Hughes, E. N., and J. T. August. 1981. Characterization of plasma membrane proteins identified by monoclonal antibodies. *J. Biol. Chem.* 256:664–671.

Hughes, E. N., A. Colombatti, and J. T. August. 1983. Murine cell surface glycoproteins. Purification of polymorphic Pgp-1 antigen and analysis of its expression on macrophages and other myeloid cells. *J. Biol. Chem.* 258:1014–1021.

Hughes, E. N., G. Mengod, and J. T. August. 1981. Murine cell surface glycoproteins. Characterization of a major component of 80,000 daltons as a polymorphic differentiation antigen of mesenchymal cells. *J. Biol. Chem.* 256:7023–7027.

Ishihara, A., B. F. Holifield, K.-E. Magnusson, and K. Jacobson. 1988. The lateral distribution of plasma membrane glycoproteins in locomoting cells. *J. Cell. Biochem.* In press.

Ishihara, A., Y. Hou, and K. Jacobson. 1987. The Thy-1 antigens exhibits rapid lateral diffusion in the plasma membrane of rodent lymphoid cells and fibroblasts. *Proc. Natl. Acad. Sci. USA.* 84:1290–1293.

Jacobson, K. 1983. Lateral diffusion in membranes. *Cell Motil.* 3:367–373.

Jacobson, K., D. O'Dell, and J. T. August. 1984*a*. Lateral diffusion of an 80,000 dalton glycoprotein in the plasma membrane of murine fibroblasts: relationships to cell structure and function. *J. Cell Biol.* 99:1624–1633.

Jacobson, K., D. O'Dell, B. Holifield, T. L. Murphy, and J. T. August. 1984 *b*. Redistribution of a major cell surface glycoprotein during cell movement. *J. Cell Biol.* 99:1613–1623.

Kapitza, H.-G., G. McGregor, and K. Jacobson. 1985. Direct measurement of lateral transport in membranes using time-resolved spatial photometry. *Proc. Natl. Acad. Sci. USA.* 82:4122–4126.

Marcus, P. I. 1962. Dynamics of surface modification in myxovirus-infected cells. *Cold Spring Harbor Symp. Quant. Biol.* 27:351–365.

Middleton, C. A. 1979. Cell-surface labeling reveals no evidence for membrane assembly and disassembly during fibroblast locomotion. *Nature (Lond.).* 282:203–205.

Murphy, T. M., G. Decker, and J. T. August. 1983. Glycoproteins of coated pits, cell junctions, and the entire cell surface revealed by monoclonal antibodies and immunoelectron microscopy. *J. Cell Biol.* 97:533–541.

Petty, H. R., and J. W. Francis. 1986. Polymorphonuclear leukocyte histamine receptors: occurrence in cell surface clusters and their redistribution during locomotion. *Proc. Natl. Acad. Sci. USA.* 83:4332–4335.

Ryan, G. B., J. Z. Borysenko, and M. J. Karnovsky. 1974. Factors affecting the redistribution of surface-bound concanavalin A on human polymorphonuclear leukocytes. *J. Cell Biol.* 62:351–365.

Trinkaus, J. P. 1985. Protrusive activity of the cell surface and the initiation of cell movement during morphogenesis. *Exp. Biol. Med.* 10:130–173.

Trowbridge, I. S., J. Lesley, R. Schulte, R. Hyman, and J. Trotter. 1982. Biochemical characterization and cellular distribution of a polymorphic, murine cell-surface glycoprotein expressed on lymphoid tissues. *Immunogenetics.* 15:299–312.

Vasiliev, J. M., I. M. Gelfand, L. V. Domnina, N. A. Dorfman, and D. Y. Pletyushkina. 1976. Active cell edge and movements of concanavalin A receptors of the surface of epithelial and fibroblastic cells. *Proc. Natl. Acad. Sci. USA.* 73:4085–4089.

Vaz, W. L. C., F. Goodsaid-Zaldaondo, and K. Jacobson. 1984. Lateral diffusion of lipids and proteins in bilayer membranes. *FEBS (Fed. Eur. Biochem. Soc.) Lett.* 174:199–207.

Walter, R. J., R. D. Berlin, and J. M. Oliver. 1980. Asymmetric F_c receptor distribution on human PMN oriented in a chemotactic gradient. *Nature (Lond.).* 286:724–725.